Iloglu, Suzan; Albert, Laura A.

Article

A maximal multiple coverage and network restoration problem for disaster recovery

Operations Research Perspectives

Provided in Cooperation with:
Elsevier

Suggested Citation: Iloglu, Suzan; Albert, Laura A. (2020) : A maximal multiple coverage and network restoration problem for disaster recovery, Operations Research Perspectives, ISSN 2214-7160, Elsevier, Amsterdam, Vol. 7, pp. 1-14, https://doi.org/10.1016/j.orp.2019.100132

This Version is available at:
https://hdl.handle.net/10419/246407

Operations Research Perspectives 7 (2020) 100132

Contents lists available at ScienceDirect

Operations Research Perspectives

journal homepage: www.elsevier.com/locate/orp

A maximal multiple coverage and network restoration problem for disaster recovery

Suzan Iloglu[a], Laura A. Albert[b,*]

[a] Yale School of Public Health, 350 George Street, New Haven, CT 06520, United States
[b] Industrial & Systems Engineering University of Wisconsin-Madison 3218 Mechanical Engineering Building, 608-262-3002, United States

ARTICLE INFO

Keywords:
OR in disaster relief
Maximal multiple coverage problem
Network restoration
Scheduling on parallel servers
Emergency response

ABSTRACT

The recovery of physically damaged infrastructure after disasters is critical to efficiently deliver disaster relief supplies and emergency services. The physical damage to road infrastructure from disasters can result in decreased road link capacities and an inability to meet the community's emergency demand. This paper provides an infrastructure restoration plan for delivering critical services after disasters. We present a maximal multiple coverage and network recovery problem for the recovery and restoration of infrastructure systems after disasters. In the model, recovery crews make damaged arcs available by repairing components over a time horizon in a disrupted network. The model relocates emergency responders using the available arcs in the network to maximize multiple coverage of emergency service demand over the time horizon. We present two heuristics for the model. The first uses the Lagrangian and the linear programming relaxation solutions of the problem, and the second uses an integer rounding procedure applied to the linear programming relaxation solution. We test the model using a real-world example representing the road infrastructure and emergency services of the Bronx Borough in New York, NY during Hurricane Sandy. The results demonstrate that the integer rounding heuristic is effective in identifying near-optimal solutions. Our computational study suggests that our model can aid emergency managers in achieving their goals by scheduling effective restoration activities for real-time disaster recovery and long-term recovery planning.

1. Introduction

After disasters, road infrastructure becomes vital for providing aid and saving disaster victims' lives, as it provides a critical link to emergency services, relief, and evacuation routes. Disaster–related disruptions on the road infrastructure system make it hard to serve emergency calls and provide emergency aid. For example, during Hurricane Sandy, more than half of the road infrastructure system was unavailable [1]. Following Hurricane Sandy, the Department of Transportation authorized $12.4 billion to repair and reopen roads and rebuild transit assets [1]. During Hurricane Harvey in 2017, many roadways suffered catastrophic flooding, which resulted in debris on roads, even major highways such as I-10, I-45 and US-59 [2]. The Texas Department of Transportation crews cleared roadways by removing more than 10 million cubic feet of debris in the areas most impacted by the hurricane [3]. Days before a hurricane reaches a coast, government agencies pre-locate emergency response resources [4,5]. During disaster response operations, the planning staff decides the priority of roads and streets to allocate local resources [6]. Given the large repair cost and extended damage to road infrastructure, prioritizing the recovery of roadways based upon their importance to emergency services is crucial. The prioritization decisions need more advanced analytical methods to improve the recovery efforts.

During normal operations, emergency responders (e.g., firefighters, police, emergency medical service (EMS) providers) have a certain service region based on travel time to respond to emergency calls [7]. However, during and immediately after disasters, emergency responders located in regions with many disrupted roads cannot respond to demand in their service areas as quickly as during normal operations. Therefore, the locations of emergency responders and the condition of the surrounding the road infrastructure system around their locations have a critical impact on the number of people that can be reached in a timely manner after disasters. The damage to road infrastructure (e.g., from debris or flooding) and the geographic features of the region may limit the movement of emergency responders. Further, first responders and other resources that are staged prior to the disaster may only be able to access certain points of the affected region after the disaster occurs [4]. As a result, not all the facility locations may be available at

* Corresponding author.
E-mail addresses: suzan.iloglu@yale.edu (S. Iloglu), laura@engr.wisc.edu (L.A. Albert).

https://doi.org/10.1016/j.orp.2019.100132
Received 19 April 2019; Received in revised form 26 November 2019; Accepted 26 November 2019
Available online 03 December 2019

the beginning of the disaster recovery operations, and they may become available as road infrastructure is dynamically restored.

We study how to optimally coordinate both road infrastructure restoration (e.g., clearing debris from roads) and emergency response efforts after disasters. The goal of the model is to maximize the multiple coverage of emergency service demand over a time horizon. Due to high volume of emergency service requests after disasters, unavailability of emergency service responders is more likely. We capture this issue by covering emergency service demands multiple times to incorporate backup coverage. In our model, we consider the road infrastructure system as a network and repair physical components of road infrastructure to restore the network. The model seeks to schedule the restoration of the road infrastructure system over a time horizon and locates emergency responders at facilities. After restoration is completed, the disrupted arcs become available in the network. Emergency responders deliver emergency relief and services more effectively by changing locations as more arcs in the network become available during the recovery process. The model considers limited entry points to the affected region after the disaster as well as restrictions on the movement of the emergency responders during the recovery process that reflect road damage or geographic limitations, two important considerations of emergency response operations. The model consists of three parts. The recovery part models component installations by identical recovery crews over a finite time horizon. The relocation part models the movement of the emergency responders using arcs that are initially available or that become available following restoration. The coverage part captures covering demand points if there are available arcs in the network to do so.

In this study, we make the following contributions:

- We present a maximal multiple coverage and network recovery problem that considers the interdependency between disaster recovery performance of the network recovery crews and emergency service responders. This model studies how to effectively cover emergency demands with backup coverage by locating and relocating emergency responders on a network, subject to relocation restrictions, while recovering a network over a finite time horizon.
- We introduce two heuristics, each of which provides a feasible solution for the problem as well as a lower bound to the optimal objective function value. The first heuristic is based on the Lagrangian relaxation solution procedure and the second heuristic is based on an integer rounding procedure for the linear programming relaxation.
- We present a detailed case study using real world data from Bronx Borough during Hurricane Sandy. We include computational studies to demonstrate the effectiveness of the heuristics. The solution sheds light on the prioritization of the network restoration and relocation activities of emergency responders after disasters to achieve better emergency demand coverage.

The remaining sections are organized as follows. Section 2 presents a literature review. Section 3 provides the mathematical formulation of our model and introduces the two heuristics, namely, the Lagrangian and linear relaxation heuristic and the linear relaxation rounding heuristic. Section 4 reports computational results obtained by using the heuristics to identify feasible solutions for our model on a realistic case study and discusses the key insights from the analysis. The model solutions identify network recovery plans and the movement of emergency responders on available arcs. In addition, the results give insights into how to relocate emergency responders subject to relocation restrictions to maximize multiple coverage of emergency service demand over the time horizon. Section 5 provides concluding remarks.

2. Literature review

We present a coverage problem that maximizes the multiple coverage of emergency service demand by locating emergency responders at facilities. Coverage problems are one of the main classes of location problems that consider coverage of service areas based on spatial proximity. Coverage models have been studied extensively by using a wide range of methodological and theoretical developments in the literature and have been applied to public service problems [8].

Toregas et al. [9] present the first *deterministic* model, the location set covering problem (LSCP), with an objective to minimize the number of facilities to cover all demand points. Given the limited number of resources, covering all demand points could be hard to achieve. Church and ReVelle [10] present the maximal covering location problem (MCLP), with the aim of maximizing coverage by locating a fixed number of facilities. However, the LSCP and the MCLP ignore facility unavailability that occurs when an emergency responder cannot cover demand points when the emergency responder is dispatched to a demand point. Several deterministic models consider the multiple coverage of demand points to capture backup coverage. Hogan and ReVelle [11] introduce a model that considers the secondary coverage of a demand node. Gendreau et al. [12] present a double coverage location model with two different coverage standards. The model requires all the demand points to be covered by an emergency responder located within r_2 time units. In addition, a proportion α of the demand must be within r_1 time units of an emergency responder with $r_1 \leq r_2$.

In addition to deterministic models, *probabilistic* models have been developed to capture facility unavailability by explicitly considering busy probabilities and reliabilities of facilities. Daskin [13] presents the maximal expected covering location problem (MEXCLP), an extension of MCLP. MEXCLP takes into account the probability that a facility is not able to cover the demand. We consider backup coverage to capture facility unavailability by considering multiple coverage instead of considering facility unavailability probabilities, which are typically hard to estimate in disaster settings.

Another stream of papers consider *dynamic* models that relocate facilities [14]. Our model considers relocations of emergency responders between facility locations to capture dynamic changes in the network due to arc installation over the time horizon. Gendreau et al. [15] present a dynamic relocation model with the objective to maximize backup coverage while minimizing relocation costs. Rajagopalan et al. [16] present another dynamic relocation model that incorporates location–specific busy probabilities as an extension to the queuing probabilistic location set covering problem [17] with multiple periods. The aim of the dynamic set covering location model in [16] is to minimize the number of emergency responders required while meeting predetermined emergency responder availability requirements for dynamic demand environments. Another dynamic model is the time–-dependent emergency responder allocation model, which captures travel time and demand site variations due to time of day [18].

Relocation is practical for firefighters and emergency responders. Therefore, most relocation models consider emergency service responders. However, a large number of relocations creates a poor work environment for personnel. Hence, the issue of controlling the number of relocations has arisen in the dynamic coverage model literature by considering relocation cost or an upper limit on the number of location changes [19]. For example, the model presented by Gendreau et al. [15] penalizes repeated relocation of the same vehicle to limit the number of relocations. Van Buuren et al. [20] present a dynamic ambulance relocation model that only allows relocation of idle emergency responders to limit the number of relocations. We consider relocations over a time horizon during a disaster recovery to capture the dynamic change in the network due to recovery. Our model installs network components to enable emergency responders to move between emergency responder locations. Since we consider the recovery efforts over a finite time horizon, decisions regarding how to invest this limited time to install components can be considered a cost of relocating.

The coverage models in all three categories have represented important contributions to location analysis and modeling in a range of

problem contexts. In addition, the existing models employ a wide range of methodological and theoretical improvements to develop better solution techniques. Church and ReVelle [10] present two different heuristics, namely the greedy adding and the greedy adding with substitution algorithms to construct feasible solutions for MCLP. Later, Galvão and ReVelle [21] solve the Lagrangian relaxation dual of MCLP using a subgradient algorithm by improving upper and lower bounds obtained from the algorithm at each iteration. We present a Lagrangian and linear relaxation heuristic and a linear relaxation rounding heuristic to construct feasible solutions for the problem. In these heuristics, we compare feasible solutions obtained using different types of neighborhood search algorithms. Vatsa and Jayaswal [22] present a formulation for a multi-period MCLP with server uncertainty. This model is efficiently solved using Benders decomposition, while a tabu search heuristic is used to identify near-optimal solutions to the models presented in [12,15]. Recently, Cordeau et al. [23] propose solving large scale maximal covering problems using branch-and-Benders-cut algorithms.

Sharkey et al. [24] present interdependency relationships between infrastructure systems to study the necessary level of coordination for effective restoration efforts across all systems after disasters. We study the interdependency between disaster recovery performance of the network recovery crews and emergency service responders. There are few papers in the literature that study interdependencies of infrastructure systems and network recovery while measuring the performance of the system over a planning horizon. Lee et al. [25] introduce the interdependent layer network (ILN) model to explicitly model infrastructure interdependencies as a network-flow based model, where interdependent infrastructure systems are networks, and corresponding services are flows. Nurre et al. [26] introduce the integrated network design and scheduling (INDS) problem to model the restoration services of interdependent infrastructure systems after disruptive events. The INDS problem allows recovery crews to install new arcs and nodes into the network with the objective to maximize the cumulative weighted flow through the network over a time horizon. The recovery part of our model has similar constraints as the model proposed in [26]. Cavdaroglu et al. [27] extend the INDS problem to multiple interdependent networks with the objective to minimize cost, which includes flow cost, unsatisfied demand cost, and arc installation and assignment costs over the planning horizon of the restoration. Almoghathawi et al. [28] present a restoration problem for interdependent infrastructure networks with the aim of maximizing the resilience of the networks while minimizing the total restoration cost. Maya Duque et al. [29] propose a network repair crew scheduling and routing problem to optimize accessibility to humanitarian relief demand areas, and the model is solved using dynamic programming. Instead of scheduling one repair crew and including precedence relationships between damaged nodes as in [29], our study considers multiple repair crews, and models the dependency between damaged components by letting several network components benefit from each installation. Recently, Morshedlou et al. [30] present an integrated vehicle routing problem and infrastructure network restoration crew scheduling problem with the objective to maximize the resiliency of the infrastructure network over a restoration time horizon. Baycik and Sharkey [31] propose interdiction-based approaches to identify damage in disrupted critical infrastructures by accounting their dependencies to develop inspection plans.

Our paper is a companion paper to [32], who formulate a component-based integrated restoration and location problem (c-IRLP) [32], an extension to the P-median problem that models the interdependency between infrastructure systems and service providers as a network. An essential distinction of our model is that we restrict initial emergency responder locations as well as relocations, whereas c-IRLP allows emergency responders to relocate anywhere on the network without restriction. In this way, the model proposed in this paper generalizes c-IRLP by lifting the assumption that all emergency responders can be located anywhere on the network at any time without restriction. Furthermore, our model considers multiple coverage of emergency service demand to provide backup emergency service during large volume of emergency service requests after disasters, whereas c-IRLP assigns the closest emergency responder to each demand location and does not take backup coverage into account.

3. The maximal multiple coverage and network recovery problem

In this section, we introduce the maximal multiple coverage and network recovery (MMCaNR) problem for recovering disrupted components in a network while relocating emergency service providers and covering demands, which we formulate as an integer programming model. In the model, we consider a network as a topological structure that consists of nodes and arcs. Nodes in the network represent emergency service demand points and emergency facility locations. Arcs represent the paths between facility locations and demand points and between facility locations. Since we consider the disrupted network after a disaster, there are impassable arcs due to debris or other types of disaster damage. Therefore, the network has disrupted arcs as well as initially available arcs.

The goal of the model is to cover emergency demands with backup coverage by coordinating the recovery activities of two types of service providers: emergency responders and road infrastructure recovery crews. This is accomplished by locating emergency responders at facilities and scheduling crews to repair components in the network over a finite time horizon. We assume disrupted arcs are comprised of one or more *components* (streets), any of which could be disrupted, rendering the arcs unavailable. A single component can be present on multiple paths, and therefore, repairing a component enables multiple disrupted arcs that share the component. Each recovery crew is scheduled to install at most one component into the network at each time period. Not all the facility locations are open at the beginning of the disaster recovery operation horizon due to the conditions of the surrounding road infrastructure, and they become available as the network is dynamically restored. To capture this dynamic change, we restrict emergency responder relocations. Therefore, emergency responders are located at initially available facilities at the beginning of the time horizon. They are relocated in the later time periods using available arcs, including the arcs that become available after a component installation that represent allowable paths for relocation. The objective is to maximize the cumulative multiple coverage over the time horizon.

Table 1 lists all the input sets and parameters. We initially start with a network $G = (I, A \cup E)$, where the nodes in G are the union of demand nodes D and facility locations J (i.e., $I = D \cup J$) and $A \cup E$ is the union of initially available arcs between demand nodes and facility locations A, and initially available arcs between facility locations E. At the beginning of the time horizon T, we let set $J_0 \subseteq J$ represent initially available emergency responder locations. We have four different types of arcs in the network, and each one is represented with a different set: initially available arcs $A \subseteq D \times J$ and disrupted arcs $A' \subseteq D \times J$ between demand nodes and facility locations, and initially available arcs $E \subseteq J \times J$ and disrupted arcs $E' \subseteq J \times J$ between facility locations that capture the paths for relocation.

The model considers component installations to make disrupted arcs in A' and E' available in the network. We do not install disrupted arcs directly, since they represent paths. A component represents a sub-path or a combination of sub-paths that is disrupted, and hence, installation of the component can enable multiple arcs that use the component. We define the set C' as a set of installable components into the network. Since installing a single component can enable arcs in A' and E' such that were disabled due to the disruption of that component, we define a set of components for each disrupted arc in A' and E'. We define a set of components $AC(i, j)$ for each $(i, j) \in A'$ such that installation of any component $c \in AC(i, j)$ enables arc (i, j) and allows us to cover demand point i by facility location j. Likewise, we define a set of components $EC(j, j')$ for each $(j, j') \in E'$ such that installation of any $c \in EC(j, j')$

Table 1
Input sets and parameters.

Sets	
I	set of nodes, with $I = D \cup J$
D	set of demand points, with $D \subseteq I$
J	set of facility locations, where $J \subseteq I$
J_0	set of facility locations that are initially open, with $J_0 \subseteq J$
A	set of arcs between demand points and facility locations that are initially available, with $A \subseteq D \times J$
A'	set of disrupted arcs between demand points and facility locations, with $A' \subseteq D \times J$
E	set of arcs between facility locations that are initially available, with $E \subseteq J \times J$
E'	set of disrupted arcs between facility locations, with $E' \subseteq J \times J$
C'	set of components that can be installed to the network
$AC(i, j)$	subset of installable components $c \in C'$ such that location j can cover the demand i after installation of component c, for every $(i, j) \in A'$, where $AC(i, j) \subseteq C'$
$EC(j, j')$	subset of installable components $c \in C'$ such that after installation of component $c \in C$ is completed emergency responders can move between j and j' in both directions for every $(j, j') \in E'$, where $EC(i, j) \subseteq C'$
u	source node
v	sink node
Parameters	
T	number of time periods
K	number of network recovery crews
p_c	processing time to install component $c \in C'$
w_{it}	demand at node $i \in D$ at time $t = 1, ..., T$
P	number of emergency responder crews to locate at facility locations
L	levels of coverage
θ_ℓ	marginal increase in coverage when covered ℓ times for $\ell = 1, ..., L$
N_i^A	subset of facility locations $j \in J$ such that location j cover the demand i using an initially available arc $(i, j) \in A$

allows emergency responders to move between facilities j and j' in either direction. Components are installed by one of the K identical network recovery crews over a finite time horizon T. We represent the component installation times with integral parameter p_c for each $c \in C'$. After the installation of component $c \in C'$ is completed: (1) if $c \in AC(i, j)$, the demand point $i \in D$ can be covered by facility location j, (2) if $c \in EC(j, j')$, the arc $(j, j') \in E'$ between facility location j and j' becomes available for emergency responder relocations. Note that a component $c \in C'$ can enable multiple disrupted arcs in A' and E'.

Fig. 1 illustrates the relationship between components and arcs with facility location 0 and demand points 1 and 2. The solid lines represent the initially available arcs that do not cover the demand points while dashed lines represent the disrupted components. In Fig. 1, c_1 and c_2 represent installable components, with component c_1 representing a short segment of the path and c_2 representing a longer segment of the path that also includes c_1. When component c_1 is repaired, a disrupted arc between facility location 0 and the demand points 1 and 2 becomes

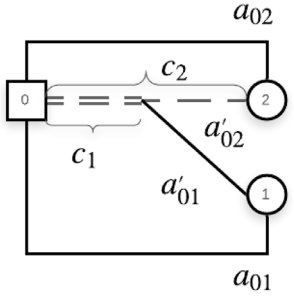

Fig. 1. The network shows components and arcs relationships with facility location 0 and two demand nodes represented with 1 and 2. The solid lines represent initially available arcs. The dashed lines represent the installable network components.

available that could allow facility location 0 to cover demand 1. When component c_2 is repaired, the disrupted arcs between facility location 0 and demand 1 and 2 become available that could allow facility location 0 to cover demands 1 and 2.

The model relocates emergency responders over a time horizon to achieve better coverage using the available arcs. If an emergency responder is located at a facility, we call that facility an "open facility." After disasters, not all facilities are open. We model emergency responder relocations over the time as network flows. To do so, we introduce a dummy source node u, which is connected by arcs to the initially open locations in J_0, and a dummy sink node v, which is connected by arcs to the locations in J. The P emergency responders are located at facilities in J_0 by moving from the dummy source node u at the beginning of the time horizon. Then emergency responders are relocated in the network at each time period using the available arcs at the time. While there is no cost for relocating emergency responders, the relocation restrictions ensure that relocation times are short. Emergency responders can move to adjacent facility locations using only available arcs. If the arcs for relocating emergency responders are defined as those whose travel times are within a certain time threshold parameter, the relocation times between any pair of facility locations are approximately the same. At the end of the time horizon, emergency responders move to the dummy sink node v.

We consider multiple coverage to respond to the large demand volume after disasters in the presence of emergency responder unavailabilities. The model considers L levels of coverage, and a demand point is fully covered if it is covered by L facilities. The objective is to maximize cumulative multiple coverage with weights w_{it} and θ_ℓ, where w_{it} represents the demand at node i at time t and θ_ℓ represents the marginal increase in coverage if covered ℓ times, $\ell = 1, ..., L$. The parameter θ_ℓ is positive and non-decreasing with $\sum_{\ell=1}^{L} \theta_\ell = 1$. The full set of input sets and parameters is listed in Table 1.

The model has three parts. The recovery part schedules the installation of the components. The relocation part relocates the emergency responders at the facility locations. The coverage part captures the multiple coverage of the emergency service demand. We have three types of binary decision variables, where each corresponds to a different part in the model.

The *relocation decision variables* are:

- $y_{j,j',t} = 1$ if an emergency responder located at j at time $t - 1$ moves to emergency responder location j', where $(j, j') \in E \cup E'$ at time $t = 1, ..., T$, and 0 otherwise.
- $y_{u,j',0} = 1$ if an emergency responder moves from dummy source node u to emergency responder location $j' \in J_0$ at time $t = 0$, and 0 otherwise.
- $y_{j,v,T+1} = 1$ if an emergency responder located at $j \in J$ at time T moves to dummy sink node v at time $t = T + 1$, and 0 otherwise.

The *coverage decision variables* are:

- $z_{i\ell t} = 1$ if demand at $i \in D$ is covered by at least ℓ levels at time $t = 1, ..., T$ for $\ell = 1, ..., L$, and 0 otherwise.
- $\delta_{ijt} = 1$ if demand $i \in D$ is covered by emergency responder facility $j \in J$ using disrupted arc $(i, j) \in A'$ that becomes available after a component installation at time $t = 1, ..., T$, and 0 otherwise.

The *recovery decision variables* are:

- $\beta_{ct} = 1$ if component $c \in C'$ is operational at time $t = 1, ..., T$, and 0 otherwise.
- $\alpha_{kct} = 1$ if network recovery crew $k = 1, ..., K$ completes the installation of component $c \in C'$ at time $t = 1, ..., T$, and 0 otherwise.

Next, we formulate the model as an integer programming model.

$$Z = \max \sum_{t=1}^{T} \sum_{\ell=1}^{L} \sum_{i \in D} w_{it} \theta_{\ell} z_{i\ell t} \tag{3.1}$$

$$\text{s. t.} \sum_{j' \in J_0} y_{u,j',0} = P \tag{3.2}$$

$$\sum_{j':(j,j') \in E \cup E'} y_{j,j',t+1} - \sum_{j':(j',j) \in E \cup E'} y_{j',j,t} = 0 \text{ for } j \in J \setminus \{u, v\} \text{ and } t = 0, \cdots, T \tag{3.3}$$

$$\sum_{j \in J} y_{j,v,T+1} = P \tag{3.4}$$

$$\sum_{j':(j',j) \in E \cup E'} y_{j',j,t} \leq 1, \text{ for } j \in J, \quad t = 1, \cdots, T \tag{3.5}$$

$$y_{j,j',t+1} \leq \sum_{c \in EC(j,j')} \beta_{ct} \text{ for } (j, j') \in E', \quad t = 1, \cdots, T \tag{3.6}$$

$$y_{j,j',t} \in \{0, 1\} \text{ for } (j, j') \in E \cup E', \quad t = 1, \cdots, T \tag{3.7}$$

$$\sum_{\ell=1}^{L} z_{i\ell t} \leq \sum_{j \in N_i^A} \sum_{j':(j',j) \in E \cup E'} y_{j',j,t} + \sum_{j:(i,j) \in A'} \delta_{ijt} \text{ for } i \in D, \quad t = 1, \cdots, T \tag{3.8}$$

$$\delta_{ijt} \leq \sum_{j':(j',j) \in E \cup E'} y_{j',j,t} \text{ for } (i, j) \in A', \quad t = 1, \cdots, T \tag{3.9}$$

$$\delta_{ijt} \leq \sum_{c \in AC(i,j)} \beta_{ct} \text{ for } (i, j) \in A', \quad t = 1, \cdots, T \tag{3.10}$$

$$\delta_{ijt} \in \{0, 1\} \text{ for } (i, j) \in A', \quad t = 1, \cdots, T \tag{3.11}$$

$$z_{i\ell t} \in \{0, 1\} \text{ for } i \in D, \ \ell = 1, \cdots, L, \quad t = 1, \cdots, T \tag{3.12}$$

$$\sum_{c \in C'} \sum_{s=t}^{\min\{T, t+p_c-1\}} \alpha_{kcs} \leq 1 \text{ for } k = 1, \cdots, K, \quad t = 1, \cdots, T \tag{3.13}$$

$$\beta_{ct} - \sum_{s=1}^{t} \sum_{k=1}^{K} \alpha_{kcs} \leq 0 \text{ for } c \in C', \quad t = 1, \cdots, T \tag{3.14}$$

$$\sum_{t=1}^{p_c} \beta_{ct} = 0 \text{ for } c \in C' \tag{3.15}$$

$$\sum_{k=1}^{K} \sum_{t=1}^{p_c} \alpha_{kct} = 0 \text{ for } c \in C' \tag{3.16}$$

$$\alpha_{kct} \in \{0, 1\}, \ \beta_{ct} \in \{0, 1\} \text{ for } c \in C', k = 1, \cdots, K, \quad t = 1, \cdots, T \tag{3.17}$$

The objective (3.1) is to maximize the cumulative multiple coverage of emergency demand over the time horizon. The relocation part consists of constraint sets (3.2)–(3.7), the coverage part consists of constraint sets (3.8)–(3.12), and the recovery part consists of constraint sets (3.13)–(3.17). Constraint set (3.6) links the relocation and recovery parts, and constraint set (3.10) links the coverage and recovery parts. Emergency responder relocations are modeled as network flow constraints in constraint sets (3.2)–(3.5) over the available arcs in the network at time period t. Constraint set (3.2) ensures that P emergency responders are located at initially available facilities in J_0 by moving from dummy source node u at time period $t = 0$, which reflects limited access points after a disaster. Constraint set (3.3) captures relocation restrictions, and it ensures flow-balance to model facility relocations between every consecutive time periods starting from time period 0 to T. Note that for every $j \in J$, $(j, j) \in E$, therefore emergency responders can stay at the same location between consecutive time periods. Constraint set (3.4) requires that P emergency responders move from open facilities to dummy sink node v at time period $T + 1$. Constraint set (3.5) ensures at most one emergency responder is located at each facility at each time period t. At each time period t, where $t = 1, \ldots, T$, the locations of the P emergency responders are given by the set $\{j' \in J: y_{j,j',t} = 1, \ (j, j') \in E \cup E'\}$. Constraint set (3.6) requires at least one component in $EC(j, j')$ to be installed for an emergency responder to move from location j to j' if there is no initially an available arc from j to j' in E. Constraint set (3.7) requires the relocation decision variables to be binary. Note that we can reformulate MMCaNR in a straightforward manner as a static emergency responder coverage location problem by simply replacing $y_{j,j',t}$ with y_j for all $j \in J$ for the case when the relocation of emergency responders is not reasonable.

Constraint set (3.8) sets the coverage level for each demand point at each time period t and ensures that for each demand $i \in D$, the total level of coverage is less then the total number of open emergency responder locations. Note that we assume θ_{ℓ} is non-decreasing over ℓ, with $\sum_{\ell=1}^{L} \theta_{\ell} = 1$. This assumption ensures that $z_{i1t} \geq z_{i2t} \geq \ldots \geq z_{i\ell t}$ for $i \in D$ and $t = 1, \ldots, T$. If θ_{ℓ} is not non-decreasing over ℓ, we must add $z_{i1t} \geq z_{i2t} \geq \ldots \geq z_{i\ell t}$ for $i \in D$ and $t = 1, \ldots, T$ as constraints to the model. To cover demand i by a facility using an initially available arc in A, the facility must have an emergency responder located at it. To cover demand i by a facility using an initially disrupted arc $(i, j) \in A'$, the arc must be available in the network by installing any component $c \in AC(i, j)$ by that time (captured by constraint set (3.10)) and the facility j must have an emergency responder located at it (captured by constraint set (3.9)), which means constraint sets (3.9) and (3.10) both need to be satisfied. Constraint sets (3.11) and (3.12) require the coverage decision variables to be binary.

Constraint set (3.13) ensures that at most one component is installed by each recovery crew in each time period, where $\alpha_{kct} = 1$ means recovery crew k starts installation of component $c \in C'$ at time $t - p_c + 1$ and finishes installation at time t. Starting from time t, this component can be used by arcs that benefit from the component. Constraint set (3.14) requires component c to be operational (i.e., $\beta_{ct} = 1$) after installation of component c is complete. Constraint sets (3.15) and (3.16) ensure that β_{ct} and α_{kct} cannot be set to one before the processing time p_c of component c. Constraint set (3.17) requires the recovery decision variables to be binary.

MMCaNR can be trivially extended to a P-median model extension with backup coverage. The P-median variation considers relocating P emergency responders into facilities as network flows while repairing disrupted components in the network over the time horizon. The objective is to minimize the total weighted distance between demand points and the L closest open facilities over the time horizon. This extends c-IRLP presented in [32] that allows for emergency responder relocations restrictions and requires multiple emergency responder assignments for each demand node.

3.1. Lagrangian and linear relaxation heuristic

We present a heuristic using Lagrangian and linear programming relaxation of MMCaNR to construct a feasible solution to MMCaNR. Lagrangian relaxation is a common method to solve combinatorial optimization problems by dualizing the constraints that make the problem “hard” to solve [33]. However, the Lagrangian relaxation solution does not satisfy the dualized constraints. We use the linear programming relaxation solution to enhance Lagrangian relaxation solution so that the resulting solution is feasible for MMCaNR.

To construct the feasible solution, we first present the Lagrangian relaxation dual problem and optimize it using a subgradient algorithm. Then we describe a procedure for constructing a feasible solution for MMCaNR using the Lagrangian relaxation dual problem solution and the linear programming relaxation solution.

We first need to choose the constraint set to dualize to generate the Lagrangian relaxation dual of MMCaNR. We apply Lagrangian relaxation to constraint set (3.10), which links the coverage part with the restoration part. The objective function in (3.1) is then equivalent to:

$$\bar{Z} = \min\left\{-\sum_{t=1}^{T}\sum_{\ell=1}^{L}\sum_{i\in D} w_{it}\theta_{\ell}z_{i\ell t}\right\}$$

under constraint sets (3.2)–(3.9) and (3.11)–(3.17), and we present the Lagrangian relaxation dual problem using objective $\bar{Z}$. Let u_{ijt} be the Lagrangian multiplier for $(i, j) \in A'$, $t = 1, ..., T$, then we define the Lagrangian relaxation problem as following:

$$L(u) = \min \left[-\sum_{t=1}^{T}\sum_{\ell=1}^{L}\sum_{i\in D} w_{it}\theta_{\ell}z_{i\ell t}\right] + \sum_{t=1}^{T}\sum_{(i,j)\in A'} u_{ijt}\left[\delta_{ijt} - \sum_{c\in AC(i,j)}\beta_{ct}\right]$$
s. t.(3.2)--(3.9) and (3.11)--(3.17)

The Lagrangian relaxation dual is:

$$\max_{u\geq 0} L(u)$$

We optimize the Lagrangian relaxation dual problem by iteratively solving the dual problem using the subgradient algorithm in [32] with the necessary changes for our model.

We now can construct a feasible solution to MMCaNR by using the similar approach in [32] by combining the Lagrangian and linear programming relaxation solutions. Let $\bar{y}$ denote values of the decision variables of the relocation part for the Lagrangian relaxation problem solution, and let $\bar{\bar{y}}$ denote values of the decision variables of relocation part for the linear programming relaxation problem solution. Then we define a set $S = \{(j, j', t): \bar{y}_{jj't} = \bar{\bar{y}}_{jj't}\}$ that consists of the indices where the y variables have the same values in the Lagrangian and linear programming relaxation solutions. We note that the variable y values whose indices belong to set S are integer. Then, we fix the values of the y variable for the indices in the set S in MMCaNR and solve MMCaNR with these fixed values. The solution yields a feasible solution for the constraint sets (3.1)–(3.17) and provides a lower bound for the optimal objective function value.

MMCaNR is NP-complete since a maximal expected coverage model variation is embedded in it. Fixing the relocation decision variables using the heuristic algorithm results in an efficient lower bound for MMCaNR. For example, in our experiments in the following section, 80–90 percent of y variables have the same values in the Lagrangian and linear programming relaxation solutions and so by fixing these values in the heuristic yields computationally efficient feasible solutions. Next, we present another heuristic algorithm using an integer rounding procedure for the linear programming relaxation of MMCaNR.

3.2. Linear relaxation rounding heuristic

Many mixed integer programming problems are successfully solved using the idea of fixing a subset of the variables in order to obtain subproblems that are easier to solve [34]. Our model includes a large number of relocation decision variables, which presents a computational challenge when solving MMCaNR. However, only a few of the relocation variables are active in the optimal solutions. To address this issue, we fix the subset of relocation decision variables to their linear relaxation solution values and form a sub–MMCaNR problem that is smaller and easier to solve than MMCaNR. Berthold [34] introduces an approach based on a relaxation enforced neighborhood search (RENS) for mixed integer nonlinear programs (MINLPs) by rounding linear and nonlinear programming relaxation solutions to construct sub–MINLPs. We use a similar approach to construct and solve sub–MMCaNR problem as in the approach by Berthold [34].

We first solve the purely continuous linear programming relaxation of MMCaNR and let $y^{\star}$ denote the linear programming relaxation solution values of the relocation decision variables y. We construct the sub–MMCaNR problem by setting the binary relocation decision variables $y_{j',j,t}$, to 0 if no emergency responder is located at j at time t in the linear programming relaxation of MMCaNR $\left(i.e., \sum_{j':(j',j)\in E\cup E'} y^{\star}_{j',j,t} = 0\right)$ as in [34]. Therefore, a neighborhood is defined by fixing the subset of relocation decision variables y values to zero. Then, we search for a feasible solution in the neighborhood by solving the sub–MMCaNR problem. The solution is feasible for MMCaNR, since the values of the fixed relocation variables in the sub–MMCaNR problem are integer in the linear programming relaxation solution and these relocation variables satisfy all of the constraints set of MMCaNR. Therefore, the resulting solution yields a lower bound on the optimal objective value to MMCaNR.

4. Computational results

In this section, we provide a case study where we apply MMCaNR and analyze computational results obtained using real data representing road infrastructure and emergency service demands for the Bronx Borough, New York, United States. We performed computations for MMCaNR and the heuristics on a computer with a 1.4 GHz Intel Core 5 Duo Processor with 4 GB of RAM. We used GUROBI 6.5.2. to solve the mixed integer programming model that was coded in Python 2.7.

We first describe the data generation process using the real world data obtained during Hurricane Sandy in the Bronx Borough. As shown in Fig. 2, the Bronx Borough data is split into $|D| = 276$ demand nodes, each of which corresponds to the center of each census tract. The data includes $|J| = 38$ total facility location nodes; 32 fire and rescue stations [35] and six hurricane evacuation centers [36]. We use exact coordinates of facility location and demand nodes. The weight w_{it} associated with each demand node $i \in D$ for $t = 1, ..., T$ reflects 311 service damage tree complaints associated with the demand node to capture the areas affected by Hurricane Sandy (October 29, 2012–November 5, 2012) multiplied by the proportional population for the associated demand node's census tract to capture the number of possible service requests. Note that we assume the weight w_{it} is fixed over the time horizon T for each demand node $i \in D$.

More than 500 miles of roadways were affected by Hurricane Sandy in New York City due to downed trees and debris on roads [37]. Hence, to approximately create the disrupted arc set, we filter only damaged tree complaints from the 311 service requests during Hurricane Sandy. The number of damaged tree complaints in the 311 service requests data vary from 1 to 29. When there are more damaged tree complaints in the same area, we are more certain that a fallen tree has disrupted an

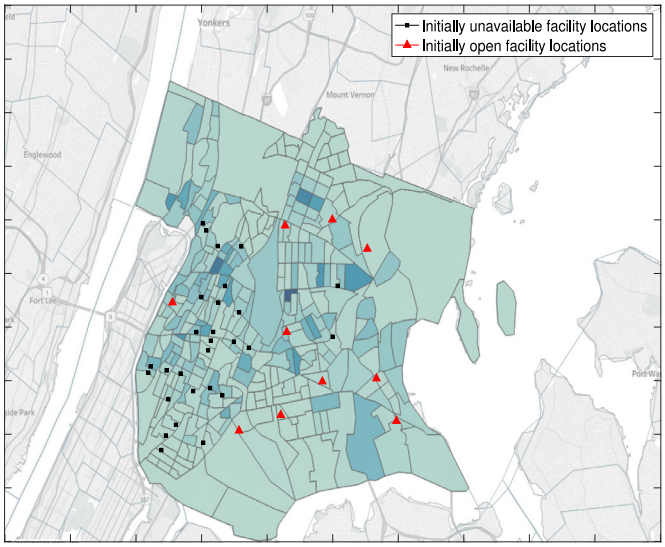

Fig. 2. Map of our case study showing initially open facility locations (in red J_0), and unavailable facility locations (in black $J\backslash J_0$). Population density is shown for each census tract of the Bronx Borough. (For interpretation of the references to color in this figure legend, the reader is referred to the web version of this article.)

arc. Therefore, if both end nodes of a component receive more than five complaints, we assume the arc, which is comprised of the component, is disrupted. Then, we filter the disrupted arcs between demand points and facility locations to the ones that only affect the coverage. To do so, we use real road distances, in miles, to decide a demand node coverage by a facility location using GeoPy package in Python. We set the coverage distance to 0.7 miles to create set A'. A coverage distance of 0.7 miles (in Manhattan distance) approximately represents three avenue blocks, which represents a walkable distance to emergency service locations in a dense urban region. According to this procedure, we generate $|A'| = 1573$ disrupted arcs between demand and facility location nodes within the coverage distance. We assume that demand–facility arcs (i, j) with fewer than five damaged tree complaints with at most one edge belong to A. Then, we generate initial coverage set N_i^A for each $i \in D$ if demand point i is within the 0.7 miles coverage distance from facility location j and $(i, j) \in A$.

We allow emergency responders relocate between facility locations if the distance between locations is less than two miles, since this represents a relocation that can be done in a short amount of time in between consecutive time periods. We generate $|E'| = 466$ disrupted arcs between facility locations with distance less than two miles. Also, we allow 10 facility locations in the coverage area (i.e., within 0.7 miles) with the least damaged tree complaints to be initially open in set J_0, since these locations represent entry points that are initially accessible to emergency responders. If each pair of facility locations j and j' are initially open, we assume there is an initially available arc (j, j') in set E. Note that for every $j \in J$, $(j, j) \in E$.

Next, we analyze the road infrastructure component-wise for disrupted arcs and create the installable component set $|C'| = 1029$. To generate sets $AC(i, j)$ and $EC(j, j')$, we first calculate up to ten shortest paths between each $(i, j) \in A'$ with distance less than or equal to 0.7 miles and $(j, j') \in E'$ with distance less than or equal to 2 miles. Then, a component belongs to set $AC(i, j)$ (or $EC(j, j')$) if at least one of the 10 shortest paths between $(i, j) \in A'$ (or $(j, j') \in E'$) becomes available following component installation. A processing time p_c for each installable component $c \in C'$ is generated by combining the real distance and damage severity that reflects the number of complaints, resulting in $1 \leq p_c \leq 10$. We allow $P = 10$ out of $|J| = 38$ facilities to be open by locating emergency responders in each time period. We set $L = 2$ to allow for primary coverage and one level of backup coverage, with $\theta_1 = 0.7$ and $\theta_2 = 0.3$. This allows for most of the benefit to come from primary coverage. Since our model considers short-term recovery of the road network components after disasters, we consider the time horizon as a day. We vary the number of time periods $T = 8, 12, 18$ to reflect the different work hours per day and the number of recovery crews $K = 1, 2, 3, 4, 5$.

We now present the results and insights obtained from solving MMCaNR. Table 2 summarizes the objective values and running times for the Bronx Borough data set for applying the heuristic algorithms and solving MMCaNR using GUROBI. The $|A'|$ and $|E'|$ columns report the number of unavailable arcs between demand–facility nodes and between facility–facility nodes, respectively. The column $|C'|$ reports the number of installable components, while column $|D|$ and $|J|$ report the number of demand nodes and facility location nodes. Column T and K report length of the time horizon and number of recovery crews. The "Linear Relaxation Rounding Heuristic Solution Value" column reports the feasible solution obtained using the integer rounding procedure and the running time in seconds in parentheses. The "Lagrangian & Linear Relaxation Heuristic Solution Value" column reports the feasible solution constructed using the Lagrangian relaxation solution and enhanced with the linear programming relaxation solution and the running time in seconds in parentheses. The "Optimal Solution Value" column reports the optimal solution and the running time in seconds in parentheses if the instance is solved optimally within an hour or the best solution values and the gap found using GUROBI within a one hour time limit. Note that reported gaps in Table 2 are the relative MIP optimality gaps found by GUROBI within an hour.

The computation time in Table 2 in the column "Linear Relaxation Rounding Heuristic Solution" includes the time to solve the linear programming relaxation. The computation time in the column "Lagrangian & Linear Relaxation Heuristic Solution" includes the time to solve the linear programming relaxation and the Lagrangian relaxation using the subgradient algorithm. Thus, the total computational times for each heuristic are comparable. We observe that the feasible solutions obtained using the linear relaxation rounding heuristic are as good as or better than the feasible solutions obtained using Lagrangian and linear relaxation heuristic in all of the instances in Table 2.

We examine the optimal solutions produced by MMCaNR by examining the performance of the model at each time period. To do so, we represent the optimal objective function value Z as a sum of the multiple coverage of emergency service demand recorded in each time period, Z_t, $t = 1, \ldots, T$, with:

$$Z_t = \sum_{\ell=1}^{L} \sum_{i \in D} w_{it} \theta_\ell z_{i\ell t}, \quad \text{for } t = 1, \ldots, T$$

and $Z = \sum_{t=1}^{T} Z_t$.

Fig. 3 reports Z_t, $t = 1, \ldots, T$ for MMCaNR instances with $K = 1, 2, 3, 4, 5$ and $T = 8$. Fig. 3 also reports the coverage values associated with a fully functional network $G^\star$, we use network $G^\star = (I, A \cup A' \cup E \cup E')$, with all arcs initially available. In $G^\star$, the P emergency responders are initially located in the initially available facilities J_0 at time $t = 0$ and are relocated over the time horizon using arcs in $E \cup E'$. The solution found using the fully functional network $G^\star$ provides an upper bound for the optimal objective function.

We report the locations of open facilities in Table 3 for $t = 0, \ldots, 8$ and $K = 5$ using the Bronx Borough data set. This allows us to compare the optimal emergency responder locations at $t = 0, \ldots, 8$ to those in the fully functional network $G^\star$.

In Fig. 3, the multiple coverage recorded using only initially available arcs at $t = 0$ is $Z_0 = 23.89$ and increases over the time horizon as the network crews install new components from C'. We observe that the model solution suggests first repairing components that enable emergency responders to move between facility locations in the network using arcs in E'. Therefore, at the earlier periods of the time horizon, coverage improvement of the system is slower and also Z_t sometimes achieves the same value for the different number of recovery crews. The difference between Z_t for $K = 1$ and $K = 2$ is significant compared to the coverage differences between other consecutive number of recovery crews. This occurs, since one recovery crew can repair one component at a time, and the first components installed tend to be in E' to enable facility locations relocations. The best possible emergency service demand coverage value occurs with the fully functional network $G^\star$. Even though the emergency responders are located at initially available facilities in J_0 at the beginning of time horizon in the network $G^\star$, relocations can occur using all arcs in $E \cup E'$, since all arcs in A' and E' are initially available. Thus the system reaches its maximal achievable Z_t value at time $t = 2$.

Fig. 4 illustrates the ratio of the multiple coverage in the optimal MMCaNR solutions (Z_t) to the corresponding multiple coverage in the same time period in the fully functional network $G^\star$, which we denote the coverage ratios. Fig. 4 illustrates the coverage ratios for $t = 1, \ldots, 8$ and $K = 1, 2, 3, 4, 5$ repair crews. The coverage ratio is 0.25 at the beginning of the time horizon at $t = 0$. When $t = 0$, all emergency responders are located at the same set of locations in J_0 in all solutions. However, the solution using the fully functional network $G^\star$ can cover significantly more demand due to all arcs in A' and E' being initially available. The coverage ratios increase between $t = 1$ and $t = 8$ as network components are repaired. Emergency managers can use this analysis to decide the number of repair crews to achieve certain ratios of coverage.

Fig. 5 provides a visual representation of the solutions for the

Table 2
Feasible and optimal solutions for the Bronx Borough data. Computational time, in seconds, is shown in the parentheses. "Linear Relaxation Rounding Heuristic Solution" reports the feasible solution value obtained using the heuristic and the computation time using GUROBI. "Lagrangian & Linear Relaxation Heuristic Solution" reports the feasible solution value obtained using the heuristic and the computation time using GUROBI and "Optimal Solution Value" reports the optimal solution if the instance is solved optimally within an hour or the best objective function value found in one hour and the computation time to solve MMCaNR using GUROBI.

$\|A'\|$	$\|E'\|$	$\|C'\|$	$\|D\|$	$\|J\|$	P	T	K	Linear relaxation rounding heuristic solution value (time(s)/gap)	Lagrangian & linear relaxation heuristic solution value (time(s)/gap)	Optimal solution value (time(s)/gap)
1573	466	1029	276	38	10	8	1	997.16(29 s)	909.83(15 s)	997.17(189 s)
1573	466	1029	276	38	10	8	2	1308.65(38 s)	1198.62(47 s)	1309.40(649 s)
1573	466	1029	276	38	10	8	3	1506.34(183 s)	1404.78 (182 s)	1506.34(913 s)
1573	466	1029	276	38	10	8	4	1643.72(48 s)	1539.47(188 s)	1646.10(533 s)
1573	466	1029	276	38	10	8	5	1744.98(43 s)	1647.35(105 s)	1744.99(1308 s)
1573	466	1029	276	38	10	12	1	1757.11(47 s)	1757.09(81 s)	1757.25(359 s)
1573	466	1029	276	38	10	12	2	2251.50(80 s)	2236.59(428 s)	2251.50(3405 s)
1573	466	1029	276	38	10	12	3	2547.83(46 s)	2445.53(187 s)	2548.84(870 s)
1573	466	1029	276	38	10	12	4	2723.87(51 s)	2723.36(135 s)	2725.73(1905.14)
1573	466	1029	276	38	10	12	5	2839.05(94 s)	2839.05(109 s)	2839.06(2177.62)
1573	466	1029	276	38	10	18	1	3046.62(424 s)	3046.70(750 s)	3046.77(3600 s/0.50%)
1573	466	1029	276	38	10	18	2	3812.17(155 s)	3811.90(624 s)	3812.17(3600 s/0.08%)
1573	466	1029	276	38	10	18	3	4179.80(518 s)	4179.80(289 s)	4180.80(3600 s/0.17%)
1573	466	1029	276	38	10	18	4	4397.01(138 s)	4396.50(310 s)	4398.87(3600 s/0.08%)
1573	466	1029	276	38	10	18	5	4538.94(197 s)	4536.63(275 s)	4538.40(3600 s/0.13%)

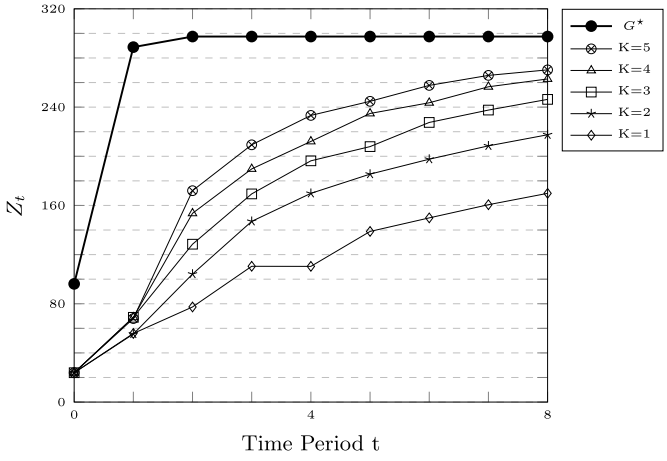

Fig. 3. Optimal multiple coverage of emergency service demand values for MMCaNR accrued in each time period for $K = 1, 2, 3, 4, 5$, and $T = 8$ for the Bronx Borough data set, where $t = 0$ represents the objective value without any repair. $G^\star$ represents the objective value when the network is fully functional and emergency responders are first located in the initially available facilities then relocated over the time horizon $T = 8$.

instance with $T = 8$ and $K = 5$ including the open facilities and their coverage areas for time periods 0, 4, and 8 as well as the solution to the instance using the fully functional network $G^\star$ at $t = 8$. Fig. 5(a) shows the initial coverage of emergency service demand and initial locations of emergency responders in the network for the optimal solution at time $t = 0$. Fig. 5(b) and (c) show the solution at time periods 4 and 8, respectively. The circles in these sub-figures illustrate the emergency responders' coverage areas. Fig. 5(d) shows the solution with the fully functional network $G^\star$.

We highlight the value of modeling relocation restrictions by comparing the optimal solutions to MMCaNR to the corresponding MMCaNR model without relocation restrictions. To do so, the set of initially available arcs between facility location is set to $E = J \times J$, and the set of disrupted arcs between emergency responder locations is set to $E' = \emptyset$. Table 4 reports the open facility locations over the time horizon for the instances of MMCaNR without relocation restrictions with $T = 8$ and $K = 5$. These locations can be compared to those in Table 3. In Table 4, the open facility locations at the beginning of the time horizon are shown in the first column represented by $t = 0$. The

Table 3
Open facility locations in the optimal solutions to MMCaNR for the Bronx Borough data set in each time period for $T = 8$ and $K = 5$. The second column $t = 0$ shows open facility locations in J_0 at the beginning of time horizon. The last column $G^\star$ shows "ideal" facility locations, which are the optimal facility locations for the fully functional network.

		Time periods t								
Facilities	$t = 0$	1	2	3	4	5	6	7	8	$G^\star$
1			×	×	×	×	×	×	×	×
5			×	×	×	×	×	×	×	
6										×
11				×	×	×	×	×	×	×
16	×	×	×	×						
18	×	×					×	×	×	×
19			×	×	×	×	×	×	×	
22		×			×	×	×	×	×	×
23						×	×	×	×	×
25		×	×	×	×	×				
26			×	×	×	×	×	×	×	×
28		×	×	×	×	×	×	×	×	×
29	×	×	×	×	×	×	×	×	×	
30	×									
31	×	×								×
34	×	×								×
35	×									
36	×	×	×	×	×					
37	×									
38	×	×	×							

last column shows the open facility locations in the fully functional network $G^\star$ at $t = 8$. In Table 4 and in the original MMCaNR instance (see Table 3), each emergency responder is relocated at most two times for a total of 10 relocations across the time horizon. In addition, Table 3 indicates that when there are relocation restrictions, there are intermediate facility locations (e.g., facility location 22) used to relocate emergency responders from one location to another if there is no direct arc to do so. There is no need for such intermediate facilities when the movement of emergency responders is unrestricted, as shown in Table 4.

We can compare the facility locations reported in Tables 3 and 4 to evaluate the relocations at each time period in the disrupted network G with relocation restrictions (Table 3) and without relocation restrictions (Table 4) as well as locations of emergency responders in the fully functional network $G^\star$. We call emergency responder locations in the

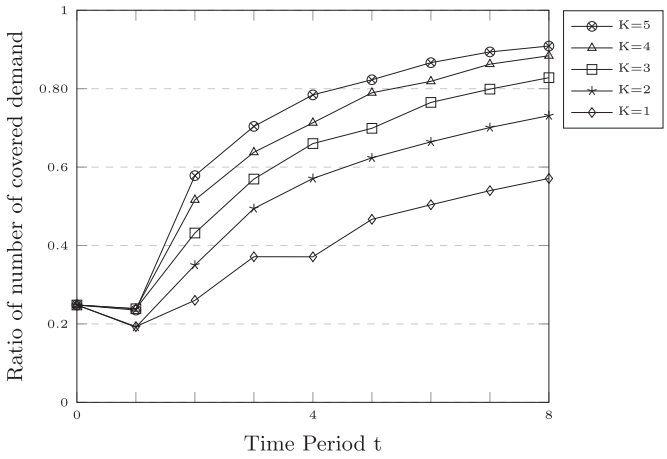

Fig. 4. Ratio of optimal multiple coverage of emergency service demand values for MMCaNR accrued in each time period for $K = 1, 2, 3, 4, 5$, and $T = 8$ compared to the optimal multiple coverage of emergency service demand values for the fully functional network $G^\star$ for the Bronx Borough data set.

final column of tables as the "ideal" emergency responder locations of the network $G^\star$, since they are the optimal facility locations in the fully functional network $G^\star$. At time $t = 8$, in Table 3, seven of the 10 emergency responder locations are the same as the "ideal" emergency responder locations in $G^\star$, and in Table 4, six of the 10 emergency responder locations are the same as the "ideal" emergency responder locations in $G^\star$. The computational results of the original MMCaNR model suggest that it is best to install components that enable disrupted arcs in E' between facility locations earlier in the time horizon and then install components that enable the disrupted arcs in A' between demand points and the open facility locations to increase the emergency service demand coverage.

Table 5 summarizes the total number of emergency responder relocations and the total distances associated with these relocations (in miles) for the instances with $T = 8$ and $K = 1, 2, 3, 4, 5$ in the original MMCaNR and the MMCaNR without relocation restrictions. We calculate the total distance of emergency responder relocations by summing the Manhattan distances between facility locations for all emergency responders over the time horizon. Note that in the original MMCaNR instances, we allow emergency responders to relocate between

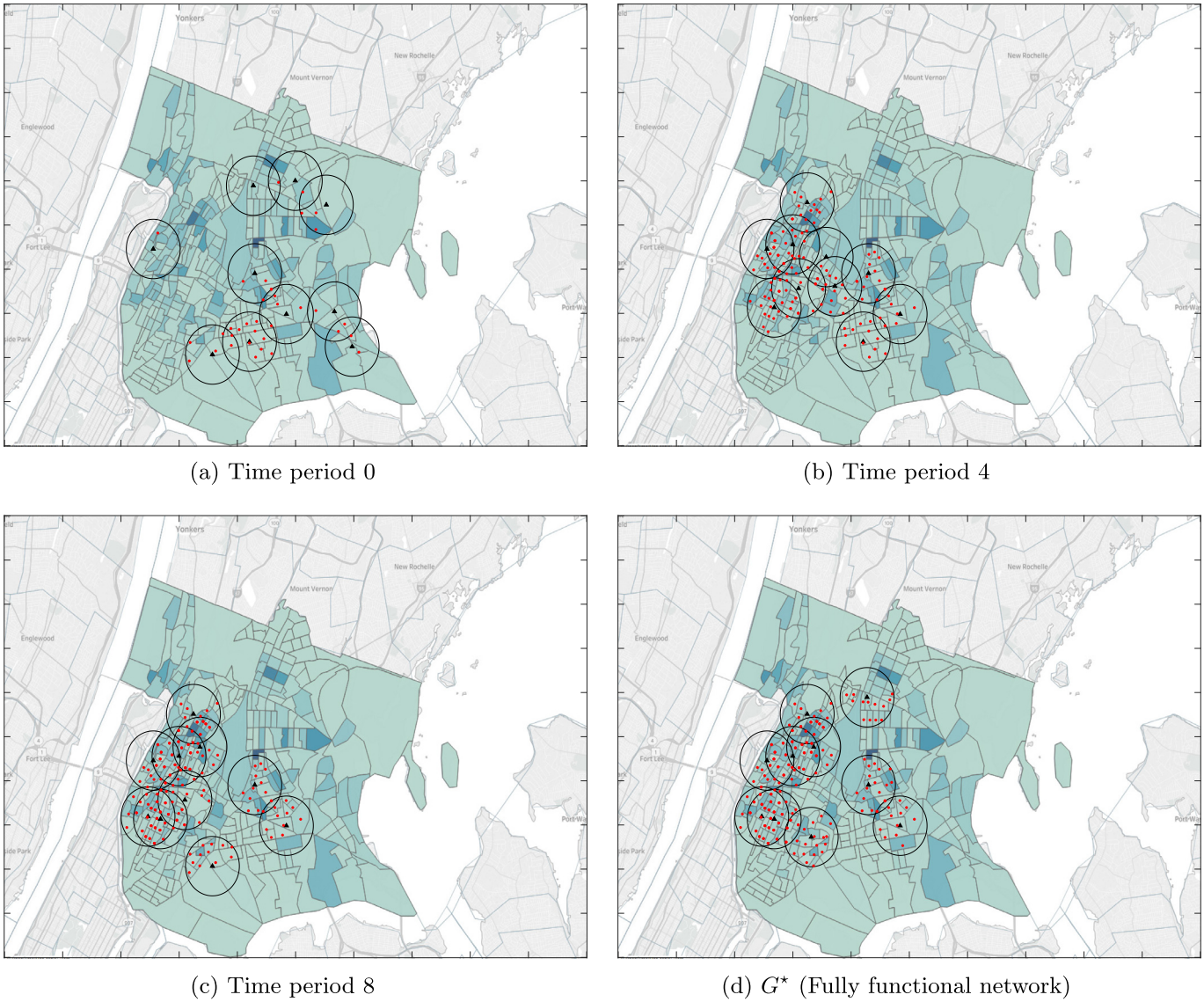

(a) Time period 0

(b) Time period 4

(c) Time period 8

(d) $G^\star$ (Fully functional network)

Fig. 5. MMCaNR emergency responder locations for the Bronx Borough data set with $K = 5$ and over the time horizon $T = 8$. (a) shows the model solution using initial arcs. The triangles represent the open facilities and the circles around them represent the coverage area of given triangles at time periods 4 and 8 in (b)–(d) shows the optimal model solution when the network is fully functional.

Table 4
Open facility locations in the optimal solutions to MMCaNR without relocation restrictions for the Bronx Borough data set in each time period for $T = 8$ and $K = 5$. The second column $t = 0$ shows open facility locations in J_0 at the beginning of time horizon. The last column $G^\star$ shows "ideal" facility locations, which are the optimal facility locations for the fully functional network.

Facilities	$t = 0$	1	2	3	4	5	6	7	8	$G^\star$
1		×	×	×	×	×	×	×	×	×
5			×	×	×	×	×	×	×	
6										×
11		×	×	×	×	×	×	×	×	×
13		×	×	×	×	×	×	×	×	
16	×	×	×							
18	×					×	×	×	×	×
19		×	×	×	×	×	×	×	×	
22				×	×	×	×	×	×	×
23										×
25		×	×	×	×					
26		×	×	×	×	×	×	×	×	×
28		×	×	×	×	×	×	×	×	×
29	×	×	×	×	×	×	×	×	×	
30	×									
31	×									×
34	×									×
35	×									
36	×	×								
37	×									
38	×									

Table 5
Comparison of the total number of relocations and the total distance of relocations (in miles) in the original MMCaNR and the MMCaNR without relocation restrictions.

	Total number of relocations		Total distance of relocations (miles)	
K	Original MMCaNR	MMCaNR with no relocation restrictions	Original MMCaNR	MMCaNR with no relocation restrictions
1	10	10	13.03	21.46
2	12	12	12.86	30.74
3	11	11	15.28	32.09
4	11	11	16.36	35.68
5	10	10	17.67	32.83

locations if there is an available arc with a distance less than or equal to two miles. Even though when we remove the relocation restrictions in the MMCaNR without relocation restrictions, the total number of relocations is similar to those of the original MMCaNR. When we remove the relocation restrictions, we observe that emergency responders travel up to six miles between consecutive time periods. Furthermore, the total distances of the relocations are more than double those of the corresponding original MMCaNR instances in three out of five instances. We further study the impact of relocation restrictions in Fig. 6, which compares the multiple coverage of emergency responders at each time period of the original MMCaNR to the MMCaNR without relocation restrictions for $K = 1, 2, 5$. We observe that there are large differences in the multiple coverage of emergency responders between the two models and that these differences are most accentuated at the beginning of the time horizon.

We perform a sensitivity analysis on various parameters of the Bronx Borough data set to understand how the original MMCaNR model solutions change under different inputs and to obtain policy insights. To do so, we create seven model instances based on the Bronx Borough data set that each change one type of input, and we solve MMCaNR with these seven additional data sets with $T = 8$ and $K = 1, 2, 3, 4, 5$. We describe these model instances as follows.

1. We consider having a different set of initially available locations J_0. Here, J_0 contains the "ideal" locations associated with the fully functional network $G^\star$, as reported last column in Table 3.
2. We consider having a different set of initially available locations J_0. Here, J_0 contains the $|P|$ most damaged facility locations, where damage is computed as the total number of 311 complaints in the location's coverage area.
3. We consider a component to be disrupted, and hence, installable if both ends of the component receive three or more complaints in the 311 data (as opposed to five complaints in the original problem instance). This results in a new installable component set C' as well as its corresponding disrupted arc set A'.
4. We set the relocation distance to one mile (two miles in the initial data set). Shortening the relocation distance changes the set of initially available arcs between facilities E and the set of disrupted arcs between facility locations E'.
5. We consider $L = 3$ levels of coverage with $\theta_1 = 0.5$, $\theta_2 = 0.3$ and $\theta_3 = 0.2$.
6. We consider a coverage distance of 1.0 mile when determining the subset of facility locations that cover demand at $i \in I$, captured by N_i^A, $i \in I$.
7. We consider locating $P = 8$ emergency responders.

We report the optimal multiple coverage of emergency service accrued in each time period for each case. The results are displayed in Table 6, Figs. 7 and 8.

Table 6 reports the objective values and running times for seven

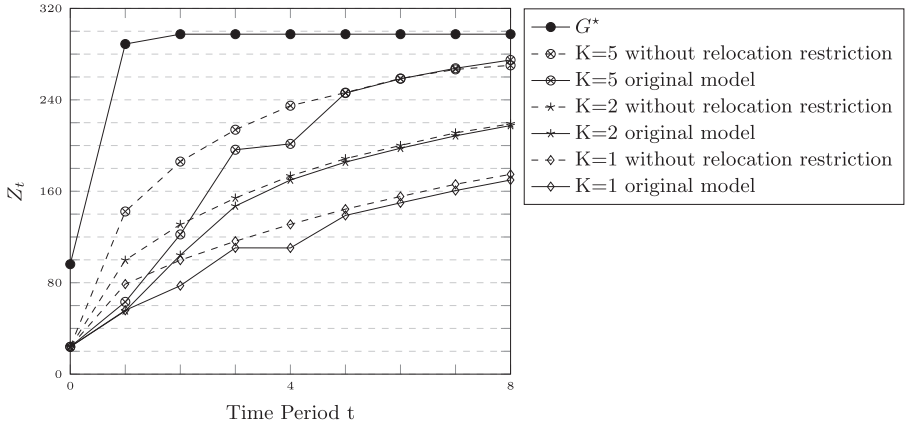

Fig. 6. Comparison of optimal multiple coverage of emergency service demand values for MMCaNR and MMCaNR without relocation restrictions accrued in each time period for $K = 1, 2, 5$, and $T = 8$ for the Bronx Borough data set, where $t = 0$ represents the objective value without any repair. $G^\star$ represents the objective value when the network is fully functional and emergency responders are first located in the initially available facilities then relocated over the time horizon $T = 8$.

Table 6
Feasible and optimal solutions for the Bronx Borough data for new instances. Computational time, in seconds, is shown in the parentheses. "Linear Relaxation Rounding Heuristic Solution" reports the feasible solution value obtained using the heuristic and the computation time using GUROBI. "Lagrangian & Linear Relaxation Heuristic Solution" reports the feasible solution value obtained using the heuristic and the computation time using GUROBI and "Optimal Solution Value" reports the optimal solution if the instance is solved optimally within an hour or the best objective function value found in one hour and the computation time to solve MMCaNR using GUROBI.

New instance name (representing figure)	T	K	Linear relaxation rounding heuristic solution value (time(s)/gap)	Lagrangian & linear relaxation heuristic solution value (time(s)/gap)	Optimal solution value (time(s)/gap)
"Ideal" locations are initially available (Fig. 7a)	8	1	1048.45 (2 s)	1038.21 (22 s)	1048.45 (19 s)
	8	2	1357.70 (15 s)	1349.11 (89 s)	1360.09 (73 s)
	8	3	1558.25 (13 s)	1557.65 (73 s)	1558.25 (210 s)
	8	4	1703.80 (9 s)	1703.80 (34 s)	1703.80 (65 s)
	8	5	1804.02 (9 s)	1804.01 (37 s)	1804.01 (63 s)
Most damaged 10 facility locations initially available (Fig. 7b)	8	1	938.80 (72 s)	930.42 (50 s)	940.60 (489 s)
	8	2	1261.58 (156 s)	1255.78 (216 s)	1261.59 (863 s)
	8	3	1471.66 (318 s)	1468.72 (580 s)	1473.70 (1880 s)
	8	4	1623.94 (351 s)	1622.18 (201 s)	1623.93 (2705 s)
	8	5	1735.80 (99 s)	1735.79 (70 s)	1735.79 (790 s)
Additional installable components(Fig. 7c)	8	1	970.52 (49 s)	970.52 (32 s)	972.57 (229 s)
	8	2	1290.85 (59 s)	1288.95 (214 s)	1292.56 (476 s)
	8	3	1492.21 (150 s)	1491.96 (74 s)	1492.21 (577 s)
	8	4	1633.38 (88 s)	1631.97 (50 s)	1633.94 (497 s)
	8	5	1733.92 (46 s)	1731.84 (48 s)	1733.92 (1038)
Relocation restriction 1 mile(Fig. 7d)	8	1	920.00 (100 s)	920.00 (40 s)	927.10 (410 s)
	8	2	1233.90 (717 s)	1232.20 (359 s)	1236.68 (2462 s)
	8	3	1441.92 (3224 s)	1439.13 (564 s)	1440.97 (3600 s/0.43%)
	8	4	1591.11 (224 s)	1591.11 (133 s)	1591.11 (1427 s)
	8	5	1691.68 (124 s)	1691.68 (70 s)	1691.68 (995 s)
Three levels of coverage(Fig. 8a)	8	1	724.63 (18 s)	718.23 (23 s)	727.15 (165 s)
	8	2	971.51 (18 s)	967.24 (69 s)	971.51 (267 s)
	8	3	1129.91 (142 s)	1129.69 (99 s)	1129.97 (689 s)
	8	4	1253.28 (85 s)	1252.19 (94 s)	1253.28 (281 s)
	8	5	1345.40 (62 s)	1344.59 (62 s)	1346.34 (404 s)
Coverage distance 1 mile (Fig. 8b)	8	1	2412.14 (270 s)	2401.93 (295 s)	2420.17 (1645 s)
	8	2	2588.38 (1804 s)	2583.85 (717 s)	2586.11 (3600 s/0.34%)
	8	3	2685.21 (1994 s)	2676.05 (2807 s)	2680.12 (3600 s/0.82%)
	8	4	2753.47 (1668 s)	2748.60 (3203 s)	2741.28 (3600 s/0.95%)
	8	5	2802.48 (2397 s)	2801.96 (1599 s)	2789.41 (3600 s/0.74%)
P = 8(Fig. 8c)	8	1	956.90 (32 s)	956.58 (30 s)	964.49 (95 s)
	8	2	1252.21 (24 s)	1250.80 (26 s)	1252.75 (230 s)
	8	3	1429.51 (36 s)	1428.41 (47 s)	1429.51 (178 s)
	8	4	1540.43 (35 s)	1536.58 (47 s)	1540.64 (595 s)
	8	5	1623.73 (118 s)	1617.75 (69 s)	1625.70 (554 s)

additional Bronx Borough data set instances, including the optimal solutions identified using GUROBI and feasible solutions identified using the two heuristic algorithms. The column labeled "New Instance Name (representing Figure)" reports the name of the new data instance with the name of the associated figure showing the multiple coverage values in each time period Z_t in parentheses. Columns T and K represent the number of time periods and number of worker crews, respectively. The last three columns report the solution value and computation times as in Table 2. We observe that in all of the experiments in Table 6, the linear relaxation rounding heuristic identifies feasible solutions that are at least as good as the Lagrangian & linear relaxation heuristic solution for all instances. This matches the observations from Table 2.

We illustrate the multiple coverage in each time period for the first four sets of model instances in Fig. 7 and for the last three sets of model instances in Fig. 8. We also compare each instance to the multiple coverage associated with its corresponding fully functional network G^*. Note that the first four sets of model instances in Fig. 7 have the same multiple coverage values associated with the fully functional network G^* at time $t = 8$ as in the original problem instance, whereas the last three sets of instances in Fig. 8 have different multiple coverage values associated with the fully functional network G^* as in the original problem instance (as shown in Fig. 3).

Fig. 7 illustrates the multiple coverage in each time period for instance sets 1–4. Fig. 7a and b illustrate the results when we change the set of initially available facility locations, J_0. Fig. 7a illustrates the case when the "ideal" locations are initially available (i.e., $J_0 = \{1, 6, 11, 18, 22, 23, 26, 30, 31, 34\}$). In this case, the total number of relocations decreases to six with $K = 5$ recovery crews and time horizon $T = 8$, since the facilities are already located in "ideal" locations. Nine of the ten open facility locations at $t = 8$ are same as those in the second last column in Table 3. Fig. 7b illustrates the case when the 10 initial facility locations are those with the most damage complaints (i.e., $J_0 = \{3, 6, 9, 10, 11, 13, 14, 20, 21, 23\}$). We observe that the multiple coverage is higher in Fig. 7b than in Fig. 3 across all time periods. This occurs, since there is a high weight at the demand points near these initially available facility locations (i.e., w_{it} values), which allows more demand to be covered without having to relocate facilities. The change in the initially open facility location set results in 10 relocations over the time horizon $T = 8$ with $K = 5$ recovery crews. When we compare the open facility locations at the end of time horizon, we observe that three are different than those in Table 3. When we compare Fig. 7a and b, we observe higher coverage in Fig. 7a for each number of repair crews K. For example, in Fig. 7a when $K = 5$, 129 demand points are covered with a primary facility and 41 demand points are covered with a backup facility, with an optimal objective function value of 1804.01 (see Table 6), while in Fig. 7b, 124 demand points are covered with a primary facility and 58 demand points are covered with a backup facility, with an optimal objective function value of 1735.79. These solutions can be compared to that of the original problem instance, which has an optimal objective function value of 1744.99 (see Table 2).

Fig. 7 c shows the multiple coverage in each time period, when we redefine the installable set of components. In this case, we have more

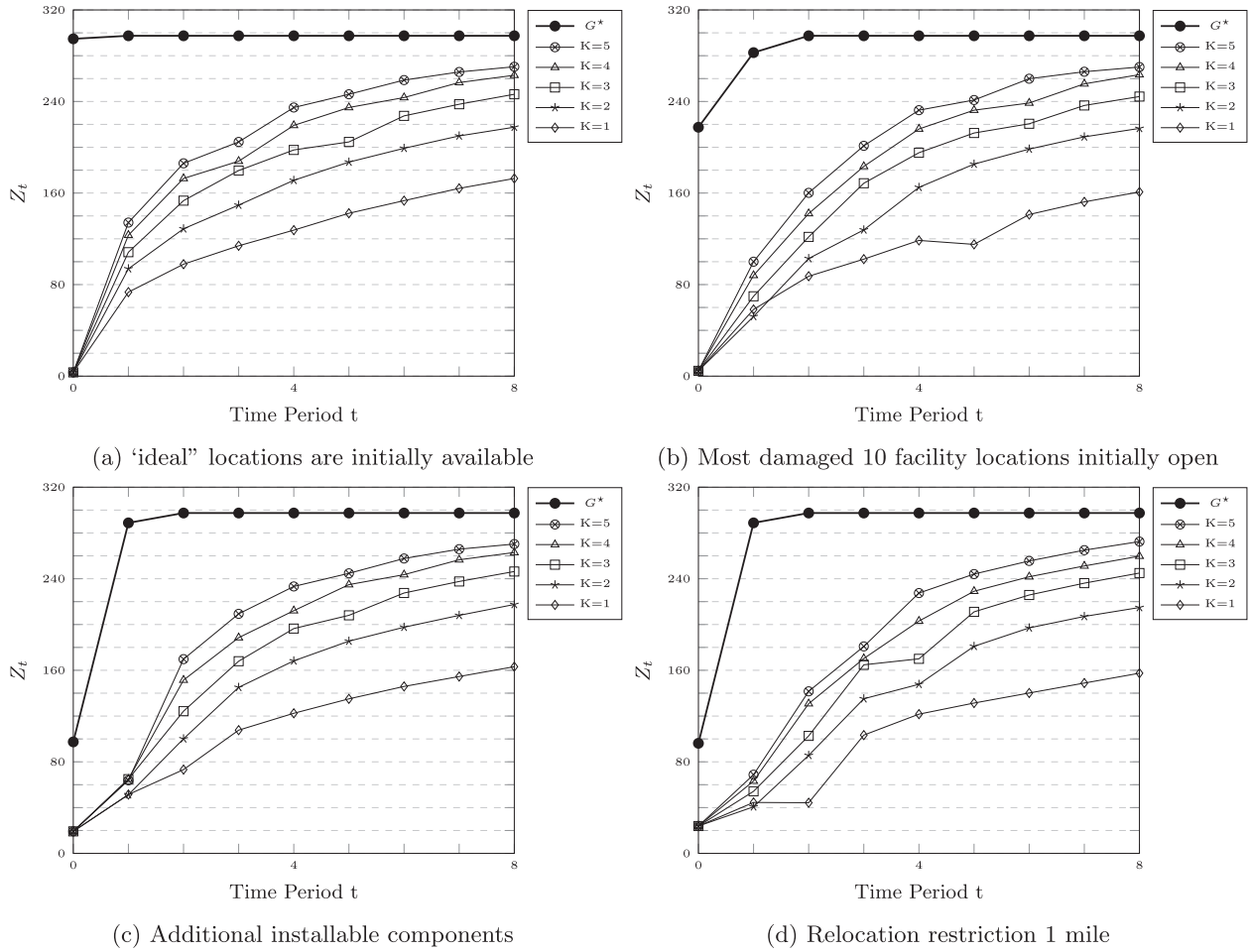

(a) 'ideal" locations are initially available

(b) Most damaged 10 facility locations initially open

(c) Additional installable components

(d) Relocation restriction 1 mile

Fig. 7. Optimal multiple coverage of emergency service demand values for MMCaNR with the different initial parameters accrued in each time period for $K = 1, 2, 3, 4, 5$, and $T = 8$ for the Bronx Borough data set, where $t = 0$ represents the objective value without any repair. $G^\star$ represents the objective value when the network is fully functional and emergency responders are first located in the initially available facilities then relocated over the time horizon $T = 8$.

installable components than in the original problem instance, reflecting more damage in the network. As a result, we observe that the multiple coverage in each time period for the given number of recovery crews is lower in some time periods than in Fig. 3. Overall, the optimal objective function values decrease by 11.07–24.6 as compared to those in the original instances (see Tables 2 and 6). At the end of time horizon $T = 8$ for $K = 5$, in Figs. 7c and 3, there are 129 demand covered with primary coverage and 42 demand with backup coverage. Fig. 7d reports the multiple coverage in each time period when we reduce the relocation distance for emergency responders to one mile (as compared to two miles in the initial data set). Reducing the relocation restriction to one mile restricts the movement of the emergency responders. As a result, the optimal objective function values decrease by 53.31–72.72 as compared to those of the original instances (see Tables 2 and 6).

Fig. 8 illustrates the multiple coverage in each time period for new instances 4–7. Fig. 8a shows the multiple coverage in each time period when we set the coverage level to $L = 3$, with primary coverage and two levels of backup coverage (as compared to two total levels of coverage in the initial data set). We set the weights to $\theta_1 = 0.5$, $\theta_2 = 0.3$ and $\theta_3 = 0.2$. We observe that nine of the ten open facilities at the end of time horizon $t = 8$ are the same as in the original data reported in Table 3. Additionally, the overall multiple coverage is lower in all time periods, since two levels of backup coverage are desired instead of one. For example, in the new instance with 3 levels of coverage and $K = 5$, there are 113 demand covered with a primary facility, 60 demand covered with a backup facility and 10 demand covered with a second backup facility. This can be compared to 129 and 42 data points covered by primary and backup facilities, respectively, in the initial problem instance. Fig. 8b shows the multiple coverage in each time period when we set the coverage distance to one mile (as compared to 0.7 miles in the initial data set). Since an open emergency responder location can cover larger area, we observe higher overall multiple coverage levels as compared to the initial data set as reported in Fig. 3. For example, with one mile coverage and $K = 5$, there are 202 demand points covered with a primary facility and 105 demand points covered with a backup facility. We observe that when we consider three levels of coverage, eight of 10 open facility locations at the end of time horizon $T = 8$ are same as the open facility locations reported in Table 3. Fig. 8c shows the multiple coverage in each time period with $P = 8$ open facility locations (as compared to $P = 10$ in the original data set). As expected, decreasing the number of open facility locations results in lower multiple coverage compared to that of the original data set as reported in Fig. 3. For example, when $T = 8$ and $K = 5$, 105 and 39 demand points are covered by a primary and backup facility, respectively. We observe that six out of eight open facility locations are same as the open facility locations reported in Table 3 at $t = 8$.

The number of recovery crews, the time horizon, and processing times of the installed components affect the number of installed components. The number of installed components affects the total number of covered demand nodes in all levels and levels of the coverage. Our computational experiments suggest that the best recovery strategy is to install components that are connected to the most critical open facility locations. Therefore, the recovery crews are relocated with the emergency responders using the available arcs in the network. Our model

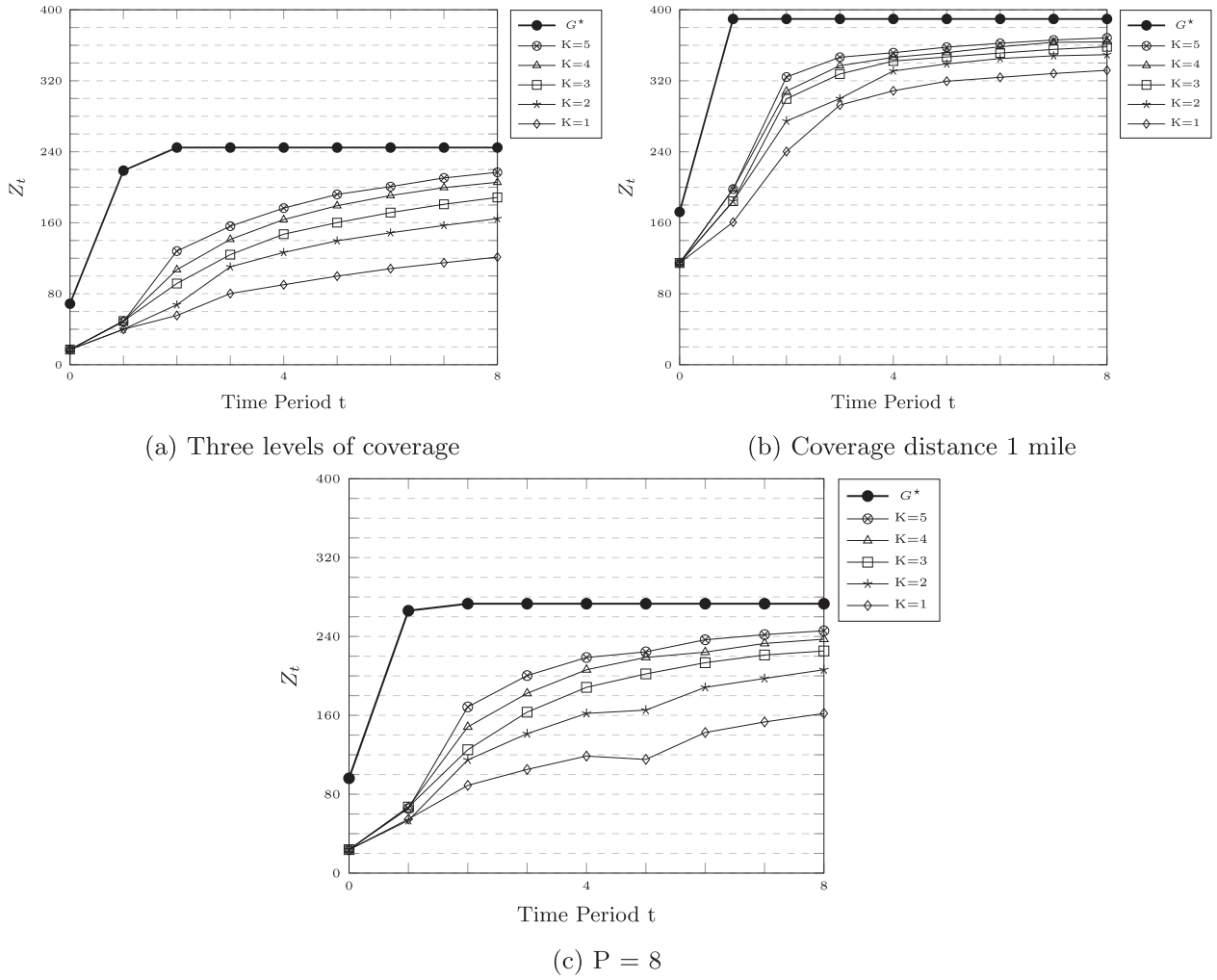

Fig. 8. Optimal multiple coverage of emergency service demand values for MMCaNR with the different initial parameters accrued in each time period for $K = 1, 2, 3, 4, 5$, and $T = 8$ for the Bronx Borough data set, where $t = 0$ represents the objective value without any repair. $G^\star$ represents the objective value when the network is fully functional and emergency responders are first located in the initially available facilities then relocated without no relocation restriction over the time horizon $T = 8$.

solutions assist decision–makers to decide the relocations of emergency responders and the schedule of recovery crews to improve the emergency service demand coverage during disaster recovery process. As a result, the solutions provide guidance to prioritize the installation of network components to deliver time–sensitive services more effectively during the disaster recovery phase.

5. Conclusions

Disruptions in road infrastructure can delay the delivery of emergency service and relief demand. In this paper, we introduce a maximal multiple coverage and network restoration problem (MMCaNR) for recovery and restoration of infrastructure systems after disasters with the goal of maximizing cumulative multiple coverage of emergency service demand over the time horizon. MMCaNR considers the interdependency between road infrastructure and emergency services. While solutions to the problem provide a plan for restoring the most critical network components, the problem also relocates emergency responders using available arcs to improve the cumulative multiple coverage of emergency service demand. Further, MMCaNR solutions can be used to measure the emergency service demand coverage after disasters.

We develop an integer programming formulation for our model. We introduce a Lagrangian and linear relaxation heuristic and a linear relaxation rounding heuristic. Each heuristic identifies a feasible solution to MMCaNR. We examine the quality of heuristics using real world data set belongs to the Bronx Borough during Hurricane Sandy. In our computational experiments, we observe that the feasible solutions obtained using the linear relaxation rounding heuristic yields better feasible solutions. These observations suggest that the model and heuristics can contribute effective emergency service demand coverage and network recovery after a disaster.

CRediT authorship contribution statement

Suzan Iloglu: Methodology, Software, Validation, Visualization, Writing - original draft, Writing - review & editing. **Laura A. Albert:** Conceptualization, Validation, Writing - original draft, Writing - review & editing, Supervision.

Declaration of Competing Interest

The authors declare that they have no known competing financial interests or personal relationships that could have appeared to influence the work reported in this paper.

Acknowledgments

This work was funded by National Science Foundation [Awards

1444219, 1541165]. The views and conclusions contained in this document are those of the authors and should not be interpreted as necessarily representing the official policies, either expressed or implied, of the National Science Foundation. The authors would like to thank Dr. Qunying Huang at the University of Wisconsin-Madison for providing the data used in the case study. The authors would also like to thank the anonymous reviewers for their valuable suggestions that resulted in significant improvements to this paper.

Supplementary material

Supplementary material associated with this article can be found, in the online version, at doi:10.1016/j.orp.2019.100132

References

[1] FEMA. Hurricane Sandy Recovery Efforts One Year Later. Tech. Rep.. Federal Emergency Management Agency; 2013. https://www.fema.gov/media-library-data/1382967173777-7411aa1b6d729a8a97e84dbba62083d8/FEMA_Sandy_One_Year_Fact_Sheet_508.pdf
[2] Blake ES, Zelinsky DA. National Hurricane Center Tropical Cyclone Report Hurricane Harvey. Tech. Rep.. National Hurricane Center; 2018. https://www.nhc.noaa.gov/data/tcr/AL092017_Harvey.pdf.
[3] Texas Department of Transportation. TxDOT Removes More Than 10 Million Cubic Feet of Debris. Tech. Rep.. Texas Department of Transportation; 2017. https://www.txdot.gov/inside-txdot/media-center/statewide-news/022-2017.html.
[4] FEMA. Emergency Management Considerations. Tech. Rep.. Federal Emergency Management Agency; 2013. https://www.fema.gov/media-library-data/20130726-1523-20490-0615/fema453_ch4.pdf.
[5] Furgate WC. Testimony Before the Committee on Transportation and Infrastructure, U.S. House of Representatives. Tech. Rep.. Federal Emergency Management Agency; 2012.
[6] FEMA. Public Assistance – Debris management guide. 2007.
[7] Swersey AJ. The deployment of police, fire, and emergency medical units. Handb Oper Res Manag Sci 1994;6:151–200.
[8] Murray AT. Maximal coverage location problem: impacts, significance, and evolution. Int Reg Sci Rev 2016;39(1):5–27.
[9] Toregas C, Swain R, ReVelle C, Bergman L. The location of emergency service facilities. Oper Res 1971;19(6):1363–73.
[10] Church R, ReVelle C. The maximal covering location problem. Papers Reg Sci Assoc 1974;32(1):101–18.
[11] Hogan K, ReVelle C. Concepts and applications of backup coverage. Manag Sci 1986;32(11):1434–44.
[12] Gendreau M, Laporte G, Semet F. Solving an ambulance location model by tabu search. Locat Sci 1997;5(2):75–88.
[13] Daskin MS. A maximum expected covering location model: formulation, properties and heuristic solution. Transp Sci 1983;17(1):48–70.
[14] Brotcorne L, Laporte G, Semet F. Ambulance location and relocation models. Eur J Oper Res 2003;147(3):451–63.
[15] Gendreau M, Laporte G, Semet F. A dynamic model and parallel tabu search heuristic for real-time ambulance relocation. Parallel Comput 2001;27(12):1641–53.
[16] Rajagopalan HK, Saydam C, Xiao J. A multiperiod set covering location model for dynamic redeployment of ambulances. Comput Oper Res 2008;35(3):814–26.
[17] Marianov V, Revelle C. The queuing probabilistic location set covering problem and some extensions. Socio Econ Plan Sci 1994;28(3):167–78.
[18] Degel D, Wiesche L, Rachuba S, Werners B. Time-dependent ambulance allocation considering data-driven empirically required coverage. Health Care Manag Sci 2015;18(4):444–58.
[19] Gendreau M, Laporte G, Semet F. The maximal expected coverage relocation problem for emergency vehicles. J Oper Res Soc 2006;57(1):22–8.
[20] Van Buuren M, van der Mei R, Aardal K, Post H. Evaluating dynamic dispatch strategies for emergency medical services: tifar simulation tool. Proceedings of the 2012 Winter Simulation Conference (WSC). Berlin, Germany: IEEE; 2012. p. 1–12.
[21] Galvão RD, ReVelle C. A Lagrangean heuristic for the maximal covering location problem. Eur J Oper Res 1996;88(1):114–23.
[22] Vatsa AK, Jayaswal S. A new formulation and benders decomposition for the multi-period maximal covering facility location problem with server uncertainty. Eur J Oper Res 2016;251(2):404–18.
[23] Cordeau J, Furini F, Ljubic I. Benders decomposition for very large scale partial set covering and maximal covering problems. Eur J Oper Res 2019;275:882–96.
[24] Sharkey TC, Cavdaroglu B, Nguyen H, Holman J, Mitchell JE, Wallace WA. Interdependent network restoration: on the value of information-sharing. Eur J Oper Res 2015;244(1):309–21.
[25] Lee EE, Mitchell JE, Wallace WA. Restoration of services in interdependent infrastructure systems: a network flows approach. IEEE Trans Syst Man Cybern Part C 2007;37(6):1303–17.
[26] Nurre SG, Cavdaroglu B, Mitchell JE, Sharkey TC, Wallace WA. Restoring infrastructure systems: an integrated network design and scheduling (INDS) problem. Eur J Oper Res 2012;223(3):794–806.
[27] Cavdaroglu B, Hammel E, Mitchell JE, Sharkey TC, Wallace WA. Integrating restoration and scheduling decisions for disrupted interdependent infrastructure systems. Ann Oper Res 2013;203(1):279–94.
[28] Almoghathawi Y, Barker K, Albert LA. Resilience-driven restoration model for interdependent infrastructure networks. Reliab Eng Syst Saf 2019;185:12–23.
[29] Maya Duque PA, Dolinskaya IS, Sörensen K. Network repair crew scheduling and routing for emergency relief distribution problem. Eur J Oper Res 2016;248(1):272–85.
[30] Morshedlou N, González AD, Barker K. Work crew routing problem for infrastructure network restoration. Transp Res Part B 2018;118:66–89.
[31] Baycik NO, Sharkey TC. Interdiction-based approaches to identify damage in disrupted critical infrastructures with dependencies. J Infrastruct Syst 2019;25(2):04019013.
[32] Iloglu S, Albert LA. An integrated network design and scheduling problem for network recovery and emergency response. Oper Res Perspect 2018;5:218–31.
[33] Fisher ML. The Lagrangian relaxation method for solving integer programming problems. Manag Sci 2004;50(12_supplement):1861–71.
[34] Berthold T. RENS: The optimal rounding. Math Progr Comput 2014;6(1):33–54.
[35] NYC OpenData. FDYN firehouse listing, 2012https://data.cityofnewyork.us/Public-Safety/FDNY-Firehouse-Listing/hc8x-tcnd. [Online; accessed November, 2017].
[36] NYC OpenData. Hurricane evacuation centers, 2013, https://data.cityofnewyork.us/Public-Safety/Hurricane-Evacuation-Centers/ayer-cga7, [Online; accessed October 11, 2017].
[37] Office of Emergency Management. New York City Hazard Mitigation Plan 2014. Tech. Rep.. Office of Emergency Management; 2014. http://www.nyc.gov/html/oem/downloads/pdf/hazard_mitigation/plan_update_2014/3.12_sandy_public_review_draft.pdf